Thermal cycling of (heated) fibre metal laminates

Muller, Bernhard; Hagenbeek, Michiel; Sinke, Jos

DOI
10.1016/j.compstruct.2016.05.020

Publication date
2016

Document Version
Accepted author manuscript

Published in
Composite Structures

Journal Title
XX(X):1–14

DOI: 10.1177/ToBeAssigned
www.sagepub.com/
SAGE

Thermal cycling of (heated) Fibre Metal Laminates

Bernhard Müller[1], Michiel Hagenbeek[1] and Jos Sinke[1]

Abstract

Fibre metal laminates with integrated heater elements have a promising potential as de- or anti-icing systems in aircraft structures. The alternating metal and composite lay-up in fibre metal laminates seems ideal for the development of a multifunctional skin with embedded heater elements. However, the long term durability needs to be carefully examined.

A unique thermal cycling setup has been designed and built to investigate the effects of thermal cycling on the material properties of GLARE (glass fibre reinforced aluminium). Peltier elements were used to provide external heating and external cooling by inverting the direction of the electrical current. With the same setup, heated GLARE samples can be internally heated using the integrated heater elements and externally cooled using the Peltier elements

Glass-fibre epoxy composite, GLARE, and heated GLARE samples have been thermal cycled for 4000, 8000 and 12000 cycles with temperature differences of 120 °C. The interlaminar shear strength (ILSS) increased by 6.9 % after 8000 cycles for the glass-fibre epoxy composite material compared to the non-cycled samples. The GLARE samples showed a maximum ILSS increase of 4.2 % after 12000 cycles. However, the heated GLARE samples showed a continuous decrease of the ILSS with a maximum decrease of 7.8 % after 12000 cycles.

Keywords

Glass-fibre epoxy composite; (heated) GLARE, thermal cycling, device design, interlaminar shear strength

Introduction

Integrated electric de-icing

Future aircraft demand state-of-art lightweight and eco-efficient systems and structures. The trend goes towards more electric aircraft to obtain these objectives. Integration of functions in an aircraft part is another way to reduce weight and obtain more efficient performance[28]. A multifunctional material or part can for instance add thermal, electrical or monitoring functions to its conventional structural function.

The thermal function is of particular interest for the leading edges of an aircraft.[2;9;18] Leading edges have to be heated to avoid atmospheric ice accumulation on the surface of the wings. Ice accumulation can alter the shape of the air foil and thus can lead to loss of aerodynamic performance. Conventional systems blow hot air from the engines through a series of ducts to the leading edge to melt the ice away. This however, requires support structures which lead to additional weight.

Embedding heater elements in FML

Fibre Metal Laminates (FMLs), such as GLARE, i. e. glass-fibre reinforced aluminium, are nowadays used on the Airbus A380.[1;32] The alternating metal and composite lay-up in FML seems ideal for the development of a multifunctional structural skin with embedded heater elements for the application in leading edges. The heater elements are protected from environmental influences by the outer aluminium layer and electrically shielded by surrounding glass-fibre epoxy layers. Numerous studies have been conducted which showed the enhanced material characteristics of GLARE over monolythic aluminium including the improved fatigue and damage tolerance.[1] Furthermore, an outstanding burn-through

[1]Structural Integrity & Composites, Delft University of Technology, Delft, The Netherlands

Corresponding author:
Bernhard Müller, Structural Integrity & Composites Delft University of Technology, Kluyverweg 1, 2629 HS Delft, The Netherlands
Email: b.muller@tudelft.nl

resistance was revealed and thermal material properties were determined.[13;19]

The effect of thermal cycling on FMLs

Many durability aspects have been investigated for FMLs.[34] Test data on thermal cycling of FML however is limited. Moreover, these tests were not performed on the FM906 high temperature curing epoxy which is currently used in heated GLARE and the number of cycles was limited and stayed below 2000.[7;24] However, with the assumption that de-icing systems are switched on twice during 20 % of all flights this could implicate a total of 36000 cycles for a regional passenger aircraft with a design life of 90000 flights. The number of cycles can easily be tenfold this number of cycles when taking into account that the system is generally switched on and off repeatedly during a de-icing scheme. Thus, thermal cycling tests which simulate the de- or anti-icing conditions of heated FMLs are needed to investigate the effects on their material properties. The (local) thermal stresses induced by thermal cycling due to the different thermal expansion coefficients could lead to material cracking and debonding at the interfaces. The thermal loading can also lead to ageing of the glass-fibre epoxy system and thus affect thermal and mechanical properties such as thermal expansion, shear strength, and fracture toughness.

Thermal cycling developments

Thermal cycling fatigue, i. e. exposing materials and structures to alternating temperatures, has been a research topic for decades.[7;10] That research focused on the effects of thermal cycling on the material characteristics and on the structural integrity of components.[17] Thermal cycling tests with different heating and cooling methods, for different heating and cooling rates and different dwell times were developed.[11;23]

Besides structural materials which are used e. g. in aircraft[7;10], thermal fatigue is also a known issue in materials for dental care[11] and electronic parts[23]. The alternating thermal loading of materials used for dental care and the combination (by bonding) of different materials combined with safety issues result in high demands on the material[27] and adhesive properties[14]. In the case of electronic parts, the investigation of thermal fatigue on the local (material) and the global (component) level is relevant.[25] The change of material characteristics is likely to change both the structural integrity and performance of (electronic) parts.

The proposed setup for (heated) FMLs

To investigate the effect of thermal cycling on (heated) FMLs an experimental setup is required which is reliable and capable to simulate flight conditions. The thermal loading conditions of heated FMLs due to flight conditions can be divided into thermal cycling due to the ascent and descent of aircraft (external cooling and heating) and thermal cycling due to (local) heating of the leading edges by de- and anti-icing measures (external cooling and internal heating).

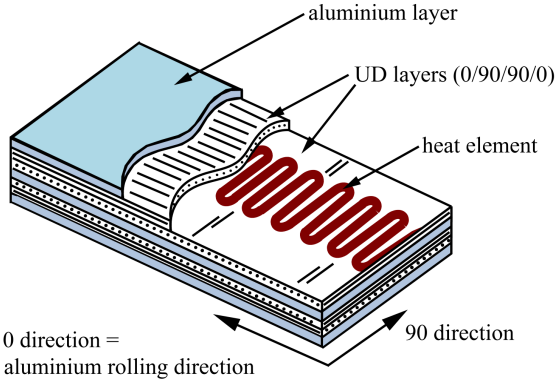

Figure 1. Schematic lay-up of a heated GLARE laminate.

The novelty of the thermal cycling setup introduced in this article is the ability to perform thermal cycling of materials with and without embedded heater elements. For structural materials the thermal cycling setup provides external cooling and external heating. For multi-functional materials (materials with embedded heater elements), the experimental setup enables thermal cycling tests by providing external cooling and internal heating. In order to simulate flight conditions, the experimental setup can be adopted to provide constant external cooling using the Peltier elements and sequential internal heating using the embedded heater elements. Furthermore, the dwell times at the minimum and maximum temperatures can be adjusted. Dwell times are used to simulate anti-icing conditions as in this case the heater elements are eventually switched on for several minutes contentiously to completely avoid icing.

In this study thermal cycling was performed on glass-fibre epoxy composites, GLARE and heated GLARE (see Figure 1) and their material properties examined before and after thermal cycling. The test results after the high number of 12000 thermal cycles, the chosen temperature ranges of 120 °C which simulate de- and anti-icing conditions and the innovation of embedding heater elements in FMLs contribute to understand the effects of thermal cyclic loads on leading edges using heated FMLs.

Heated GLARE

The heated GLARE lay-up

Heated GLARE is a FML with an embedded copper mesh between the unidirectional (UD) prepreg layers.[9] To enhance the de- and anti-icing capabilities of leading edges, the copper mesh is positioned between the UD layers which are directly underneath, i. e. as close as possible to the outer aluminium layer in the heated GLARE laminate. Figure 1 shows the schematic lay-up of this multi-functional FML. In the conventional GLARE configurations FM94 glass-fibre prepreg is used. The stiffness of this 120 °C curing epoxy system decreases significantly at temperatures beyond 70 °C.[13] In heated GLARE therefore FM906 glass-fibre prepreg is used, which is a 180 °C curing epoxy system with a T_g of 135 °C and estimated maximum service temperature of 120 °C. In combination with aluminium 7475T761 the FM906 is used as high static strength (HSS) GLARE with improved strength and service temperatures over the standard GLARE[22].

Mechanical and thermal stresses are expected to be present in heated FMLs during their service time in leading edges. Thermal residual stresses develop due to different thermal expansion of the individual materials after curing.[12] Moreover, residual stresses can result from forming processes like bending[29]. These stresses are superimposed with the mechanical and thermal service loads which appear at leading edges.

Thermal loading conditions

Figure 2 shows the expected thermal loading conditions of heated GLARE laminates which are used as anti- or de-icing devices (light brown beams) and the thermal loading conditions which were realised (red beams) in this article. Furthermore, Figure 2 depicts the lower and upper limit of the service temperature of the glass-fibre epoxy FM906 and its curing temperature. Moreover, the temperature at which ageing effects and a considerable reduction of the material properties of aluminium are expected are indicated.[26;30] Above approximately 140 °C ageing can cause moderate effect on the mechanical properties of the aluminium after a total exposure time in the order of weeks. Above approximately 200 °C the aluminium stiffness decreases more significantly and ageing happens faster.[26;30]

The first major thermal loading happens during the manufacturing process in the autoclave where the epoxy layers are cured at 180 °C for one hour and a pressure of 6 bar. The temperature increase and decrease rates in the autoclave are +2 °C/min and -2 °C/min.[13] After manufacturing, the next major thermal loading of heated GLARE is expected to happen during the service of the aircraft.

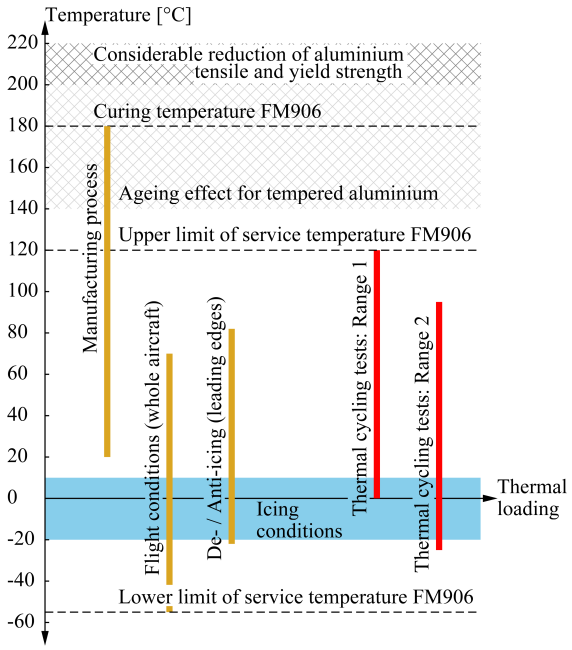

Figure 2. Major thermal loading conditions of heated leading edges made of heated GLARE[19]

Two major thermal loading conditions occur during the service of an aircraft.[19] One is the thermal cyclic loading of the whole airplane during its ascents and descents, i. e. one cycle per flight with a (service) temperature range between -55 °C and +70 °C.[31] The second thermal cyclic loading condition with a temperature range of -20 °C and +80 °C is specific for heated leading edges used as local anti- and de-icing devices.[8;18] Depending on the regional weather conditions, the number of thermal cycles are between zero and an estimated 36000 cycles as indicated in the introduction.

The thermal cycling machine

Design requirements and strategy

In the previous section the opportunities of the innovation of heated FMLs, i. e. heated GLARE were elaborated. In order to use heated FMLs in aircraft structures, their resistance to thermal and mechanical fatigue loadings needs to be investigated. Furthermore, the effect of the heater mesh on the material properties before and after thermal cyclic loading needs to be assessed. Hence, a dedicated thermal cycling machine is needed which can provide the expected temperature ranges during the anti- or de-icing device is switched on and can thermally cycle materials with (heated GLARE) and without (GLARE) heater elements to assess the effect of the heater mesh. Figure 3 a depicts the design

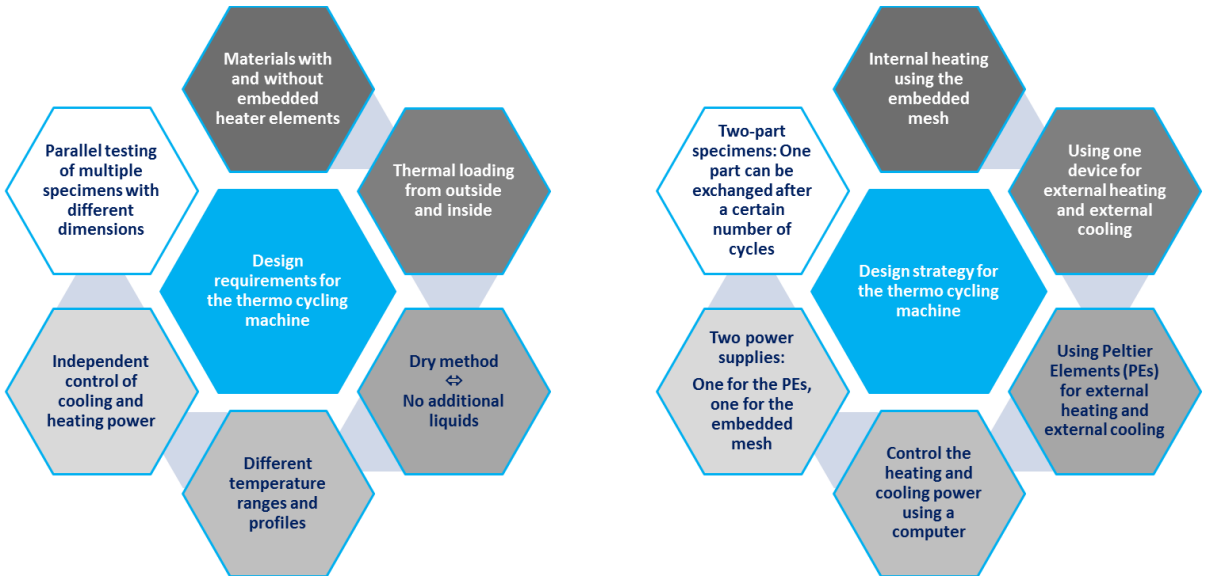

Figure 3. Thermal cycling machine: (a) Design requirements and (b) design strategy (start at the top, proceed clockwise)

requirements and Figure 3 b shows the design strategy of the developed thermal cycling machine.

Starting at the top hexagon in Figure 3 a, the first requirement of the thermal cycling machine was to allow thermal cycling of both conventional GLARE and heated GLARE. The requirement which follows instantly is the option to apply thermal loading from outside and inside. In order to fulfill these requirement it is necessary that the thermal cycling machine allows for internal heating using the embedded mesh, external heating and external cooling (cf. Figure 3 b). Providing for internal cooling is not relevant for de- or anti-icing systems.

Another requirement was to avoid a significant change of the moisture content due to thermal cycling tests, i. e. no additional liquids should get in contact with the samples. Since, the moisture content of samples can change when alternately putting them in baths with different temperatures or flushing (cooling) liquids directly on them. This requirement follows from the intention to thermally cycle glass-fibre epoxy samples (without aluminium plates on both sides) which enables the investigation of each different material layer of FMLs separately. As the glass-fibre epoxy composites are sensitive to moisture uptake and the possible effects of moderate temperatures are expected to be most significant for them[21]. The aluminium in GLARE however effectively shields of the prepreg layers and moisture absorption is therefore limited to free edges or rivet hole edges in the Glare laminate.[32] The effect of hygrothermal conditioning on FMLs is therefore much lower and often negligible.[4;5] This requirement was solved using Peltier Elements for external heating and external cooling. Peltier Elements do not introduce additional liquids and it is possible to heat and cool with the same surface by simply changing the direction of the current.[33]

The requirement to enable different minimal and maximal temperatures, temperature ranges and profiles is solved by controlling the heating and cooling power for the peltier elements by a computer, i. e. the software LabVIEW and by using a second (separate) power supply for the internal heating. Using two power supplies (one for the Peltier Elements and one for the embedded mesh) leads to a feature which makes the thermal cycling machine unique: Anti- and de-icing conditions of heated leading edges can be simulated. This can be done by switching the external cooling on (constant cooling power) and frequently the internal heating on and off. Thus, with this setting, the thermal loading conditions resulting from the cold air are simulated by the external cooling using the Peltier Elements. For the internal heating, i. e. to simulate de- or anti-icing conditions, the same embedded mesh is used.

The last design requirement was to enable the testing of multiple samples at the same time. This requirement results from the idea that if several samples are cycled at the same time, the thermal cycling machine could be used more efficiently, because after a predefined number of cycles one sample can be exchanged with another yet non-cycled sample. This is advantageous as if e. g. a maximal number of $i = j + k$ cycles is required, by cycling two samples at the same time, exchanging one sample and replacing it with another, the results after j cycles and k cycles could be examined as well. Figure 4 depicts such a sample with

two parts where the sample 1 remains in the thermal cycling machine during the whole i cycles, the sample 2 a is replace with the sample 2 b after k cycles. Thus, within the time which is needed to realise the number of i cycles, three different samples were cycled for j, k and i which equals a reduction of the overall test time by two.

The dimensions of the samples depicted in Figure 4 result from the need to conduct extensive destructive and non-destructive tests before and after thermal cycling and from the dimensions of the used Peltier Elements (50 mm x 50 mm). With the chosen sample dimension specimens can be cut for e. g. interlaminar shear strength (ILSS) tests, heat capacity test and microscopy investigations. ILSS tests are the preferred coupon tests as they test the material properties of the glass-fibre epoxy layers and the bond strength between the aluminium, the embedded mesh and glass-fibre epoxy layers at the same time. As the glass-fibre epoxy layers and the glass-fibre epoxy interfaces are the positions where possible defects or changes in the microstructure are expected.

Experimental setup

Integrating all desribed requirements led to the design of the thermal cycling machine which is shown in the Figures 5 and 6. The exploded view shows the main elements of the thermal cycling machine consisting of the support structures (frame constructions between the table, ventilators and heat sinks) and the core part of the machine. The core part of the thermal cycling machine consists of the specimens which are embedded at the top and the bottom surfaces between aluminium foil, Peltier elements and heat sinks. The temperatures (thermocouples) and the electrical power (relay, power supplies PS 1 and PS 2) of the core part are monitored and controlled by the computer (PC).

The task of the core part of the thermal cycling machine is to actually conduct the thermal cycling of the specimens. Figure 5 shows that in the introduced setup four Peltier elements at top and bottom surfaces of specimens are used for the external heating and external cooling. The four Peltier elements of the top and bottom side respectively, are connected in series. Those two circuits are switched parallel and connected to the power supply 1 (PS 1). For the case that the internal heating option of the samples is required, a second power supply (PS 2) is directly connected to the heater mesh.

The computer (PC) directly controls and monitors the amperage and voltage of both power supplies. Furthermore, the computer controls the direction of the electrical current of the Peltier elements by switching the relay which is installed between those components (cf. Figure 6). The direction of the electrical current needs to be switched to change the side at which the Peltier elements cool and heat respectively.[33] The computer uses a LabVIEW program

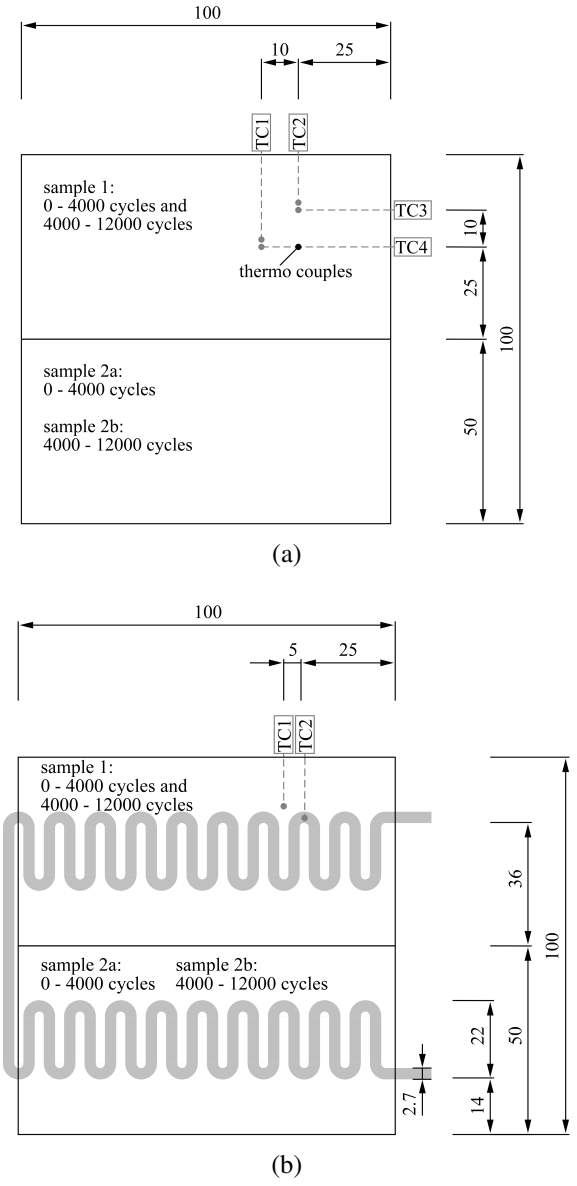

Figure 4. Sample dimensions and arrangement of the samples 1, 2a and 2b for materials (a) without and (b) with heater mesh

where it can be defined if external heating and external cooling, internal heating and external cooling or internal heating and constant external cooling (flying conditions) are executed. The maximum output amperage and voltage for both power supplies are defined in the program too. Furthermore, it is possible to adjust the dwell times at the minimum and maximum temperatures to simulate anti-icing conditions.

The computer switches the power supplies and the relay on the basis of the temperatures measured by the thermocouples (TCs) which are also recorded by the

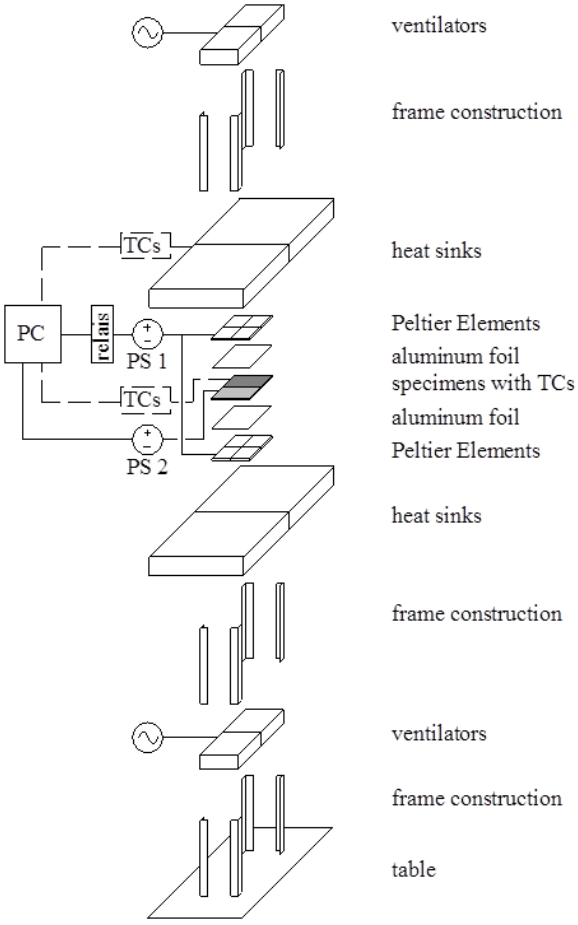

Figure 5. Exploded view of the thermal cycling machine

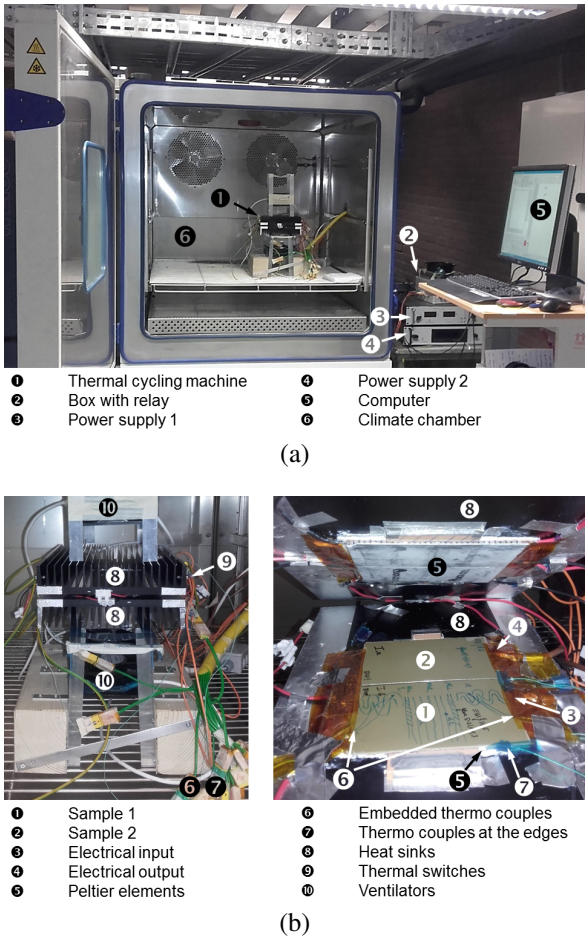

Figure 6. Photos of the thermal cycling machine in the climate chamber (a) overview and (b) detail.

computer. Thermocouples are positioned on the heat sink and embedded in the samples. Figure 4 shows the in-plane positions of the thermocouples. In the out-of-plane (thickness) direction, the thermocouples are positioned at $0.25\,t \equiv 0.55$ mm (TC1), $0.5\,t \equiv 1.1$ mm (TC2, TC4) and $0.75\,t \equiv 1.65$ mm (TC3). The variable t is the sample thickness.

The computer switches the power supplies off if a certain previously defined temperature level or the maximum cooling/heating time is reached. The thermocouple which is applied on one heat sink is used to monitor the temperature changes of the heat sink and to avoid overheating of the core part. Furthermore, temperature switches are applied on the heat sinks which mechanically switch off all power supplies in case the system overheats. Overheating of the system can happen if components fail due to the intensive usage of the whole setup or the cooling power of the Peltier elements is chosen too high in respect to the amount of heat which can be transferred to the surrounding air. [19]

The support structures have to fulfill two main tasks. The first one is to transfer the mechanical loads (weight forces) to the table and ensure stable testing conditions. This task is addressed by the frame constructions. The second task is to accelerate the heat transfer from the heat sinks to the (surrounding) air. For this, ventilators constantly blow air on the heat sinks and thereby increase the heat transfer using forced convection.

Due to the compact dimensions of the thermal cycling machine, the support structures and the core part can be placed in a climate chamber as shown in Figure 6. Placing the thermal cycling machine in a climate chamber with set temperatures lower than the ambient temperatures has the advantage that lower temperatures can be reached on the cold side of the Peltier elements. As Peltier elements generate temperature differences between their top and bottom sides, but no absolute temperatures when electrical power (DC) is applied. Hence, the temperature range at which the specimens depends on the surrounding (heat sink) temperatures can be enlarged by placing the thermal cycling machine in a climate chamber with a constant (low) temperature. Another way to extend the temperature ranges

is to stack Peltier elements, i. e. to increase the temperature differences between top and bottom sides of the stacked Peltier elements.[6]

Thermal cycling experiments and test data

Thermal cycling experiments

Thermal cycling experiments were conducted to show the functionality of the thermal cycling machine to thermally cycle materials with and without heater elements and to examine possible effects of cyclic thermal loading on the material properties of (heated) GLARE. For this, six glass-fibre epoxy samples with 16 FM906 prepreg layers, three GLARE 5-4/3-0.3 samples and three heated GLARE 5-2/1-0.3 samples were cycled thermally. The samples had thicknesses of 2.2 mm (glass-fibre epoxy), 2.3 mm (GLARE 5-4/3-0.3) and 1.2 mm (heated GLARE 5-2/1-0.3). Using two instead of three aluminum layers for the heated GLARE sample resulted from the intention to position the heater elements in the center plane in order to avoid bending moments due to non-symmetric temperature distributions through the thickness[2].

Table 1 shows the nomenclature, the materials and the layups (cf. section Heated GLARE). The abbreviations GE, GL and HG stand for glass-fibre epoxy, GLARE and heated GLARE. Furthermore, Table 1 shows the minimum and maximum set point temperatures which were supposed to be reached at the embedded thermocouples during thermal cycling and the number of thermal cycles (cf. Figure 4). The temperatures which were summed up in respect to time were recorded with the thermocouple TC3 at $0.25\,t$ for the specimens without heater elements and with the thermocouple TC2 for the heated GLARE specimen. The non-cycled samples were used as a reference to evaluate the possible effects of thermal cycling.

The minimum and maximum set point temperatures were chosen according to the expected loading conditions depicted in Figure 2. The aim of the thermal cycling range one was to test the possible effects on the glass-fibre epoxy layers when the maximum service temperature of 120°C (FM906) was reached. The minimum temperature of the thermal cycling range one was chosen with 0°C in order to use same temperature difference of 120°C for both temperature ranges. As the minimum temperature of the thermal cycling range two was chosen with -25°C and the maximum temperature with $+95$°C. The aim of the thermal cycling range two was to simulate the possible effects on the glass-fibre epoxy and on (heated) GLARE during icing conditions. The minimum and maximum temperatures for the thermal cycling range two exceeded the expected icing and de-icing conditions ± 5 °C to ± 10 °C to assure that possible heating overshoots and extreme cold icing conditions are included in the temperature range.

Table 1. Samples: Nomenclature (nom), materials, thermal loading conditions and number of cycles (noc).

nom	Material & layup	T_{min} [°C]	T_{max} [°C]	noc [-]
GE0	FM906 $(0/90/90/0)_{2s}$	na	na	0
GE1	FM906 $(0/90/90/0)_{2s}$	-25	95	4000
GE2	FM906 $(0/90/90/0)_{2s}$	-25	95	8000
GE3	FM906 $(0/90/90/0)_{2s}$	-25	95	12000
GE4	FM906 $(0/90/90/0)_{2s}$	0	120	4000
GE5	FM906 $(0/90/90/0)_{2s}$	0	120	8000
GE6	FM906 $(0/90/90/0)_{2s}$	0	120	12000
GL0	GLARE 5-3/2-0.3	na	na	0
GL1	GLARE 5-3/2-0.3	-25	95	4000
GL2	GLARE 5-3/2-0.3	-25	95	8000
GL3	GLARE 5-3/2-0.3	-25	95	12000
HG0	heated GLARE 5-2/1-0.3	na	na	0
HG1	heated GLARE 5-2/1-0.3	-25	95	4000
HG2	heated GLARE 5-2/1-0.3	-25	95	8000
HG3	heated GLARE 5-2/1-0.3	-25	95	12000

All thermal cycling experiments were conducted for 4000, 8000, and 12000 cycles. The maximum number of 12000 cycles reflects one third of the number of expected thermal cycles (cf. section Introduction) and is a significant amount of cycles which exceeds the number of previous studies[7;24]. Furthermore, the evolution of the possible material changes were tested at different times, i. e. every 4000 cycles (cf. sample 2a and 2 b in Figure 4).

Figure 7 depicts typical temperature curves measured by the embedded thermocouples (see Figure 4). Table 2 shows the summed up time intervals at the thermocouple with the maximum temperatures for 12000 cycles at which the samples were exposed to certain temperature ranges with ten degree steps.

The thermocouple with the name heat sink is applied at one of the top heat sinks to control the heat sink temperature. Thus, to avoid overheating of the machine and to assure that the cooling and heating rates keep at a constant level.[19] Hence, all four subplots of Figure 7 show an almost constant heat sink temperature, i. e. a the amount of heat which is generated by the Peltier elements and the internal mesh can be transferred to the ambient air.

The maximum cooling and heating power were defined for all thermal cycling experiments with the aim to realise the maximum thermal cycling frequency using the current test setup without overheating it. For the glass-fibre epoxy samples GE4 to GE6, the test setup was placed outside the climate chamber. Hence, the surrounding air had a temperature of $+24.5 \pm 0.5$°C. The Amperage and Voltage during the heating cycle were 12.8 ± 0.2 A and 30 ± 1 V. During the cooling cycle they were 11.8 ± 0.2 A and 30 ± 1 V. The resulting time per thermal cycle was less than 60 s.

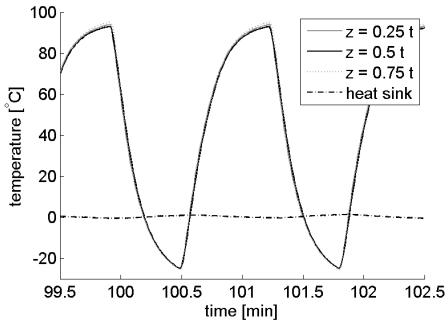

(a)

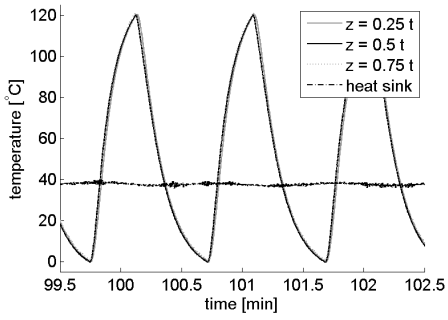

(b)

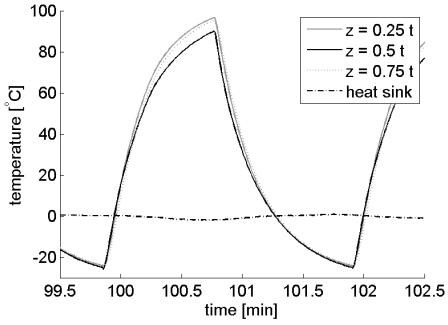

(c)

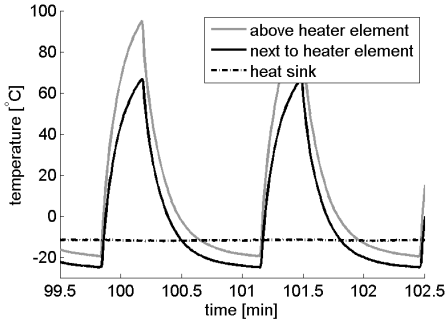

(d)

Figure 7. Typical thermal cycles of (a) GE1 to GE3, (b) GE4 to GE6, (c) GL1 to GL3 and (d) HG1 to HG3 (cf. Table 1)

Table 2. Total time in hours of the specimens which were exposed to 12000 thermal cycles (cf. Figure 7).

temp. [°C]	GE1-3 [h]	GE4-6 [h]	GL1-3 [h]	HG1-3 [h].
-30 to -20	26.7	-	55.0	11.7
-20 to -10	26.7	-	55.0	110.0
-10 to 0	20.0	-	38.3	41.7
0 to 10	15.0	38.0	26.7	25.0
10 to 20	11.7	22.0	25.0	15.0
20 to 30	13.3	15.3	23.3	15.0
30 to 40	11.7	12.7	21.7	11.7
40 to 50	11.7	10.7	23.3	10.0
50 to 60	13.3	10.0	20.0	8.3
60 to 70	15.0	10.0	30.0	6.7
70 to 80	18.3	10.3	36.7	3.3
80 to 90	33.3	10.3	55.0	2.8
90 to 100	45.0	12.3	1.7	1.9
100 to 110	-	14.7	-	-
110 to 120	-	25.0	-	-
Σ	262,7	191,3	411.7	263.1

For the thermal cycling experiments of the glass-fibre epoxy samples GE1 to GE3, the GLARE samples GL1 to GL3 and the heated GLARE samples HG1 to HG3, the test setup was moved to the climate chamber with an ambient temperature of $-15°$C to reach the minimum temperature of $-25°$C (cf. Figure 6). The Amperage and Voltage during the heating cycle for the GE1 to GE3 and the GL1 to GL3 samples were 12.8 ± 0.2 A and 30 ± 1 V and during the cooling cycle 12.8 ± 0.2 A and 35 ± 1 V. The resulting time per thermal cycle for the samples GE1 to GE3 was about 80 s and for the samples GL1 to GL3 was 120 s.

The heating power during thermally cycling of the heated GLARE samples, i. e. the sum of both samples, was $27\ \text{A} \cdot 11.1\ \text{V} = 299.7$ W. Hence, the resistance of the heater mesh(es) was $0.41\ \Omega$. For the $2 \cdot (0.1\ \text{m} \cdot 0.05\ \text{m})$ large samples, this equals a heating power of 30 kW/m^2. When subtracting the unheated edge strips of the samples, the applied heating power is close to the heating power of 34 kW/m^2 which is recommended in the literature for electrically heated leading edges[15]. The maximum Amperage and Voltage for the cooling cycles without overheating the system were 10.5 ± 0.5 A and 32 V. The applied cooling power was a little less compared to the GLARE sample as the heat sinks were not cooled by the Peltier elements during the heating cycle due to the use of internal heating. The resulting time per thermal cycle was about 80 s.

The Figures 7 a-c show that the temperature distribution through the thickness, i. e. the temperature differences between the thermocouples at $z = 0.25\ t$, $z = 0.5\ t$ and $z = 0.75\ t$, of the glass-fibre epoxy samples during the thermal cycling is less than for the GLARE samples with a similar thickness. The temperature differences between

those thermocouples embedded between different layers lies between 0 °C and 4 °C for the glass-fibre epoxy samples and between 0 °C and 7 °C for the GLARE samples. The reason for this is the higher heat capacity of aluminium compared to the glass-fibre prepeg layers.[13] Thus, more energy is required for cooling and heating the GLARE samples. The in-plane temperature distributions of the glass-fibre epoxy and GLARE samples were constant with the magnitudes according to Figures 7 a-c.

The in- and out-of-plane temperature distributions of the heated GLARE samples change with time as the heating was realised by using the internal mesh with a recurring s-shape (see Figure 4 b). Hence, the temperature differences in the samples are higher (cf. Figure 7 d). The temperatures measured directly above the heater element with one prepreg layer in between differs during the heating phase up to 15 °C to the temperatures measured 5 mm next to the heater element in the same layer where the heater elements are positioned (centre plane). During the cooling cycle the temperature distribution becomes more uniform again due to the use of the Peltier elements for external cooling.

Table 2 gives the total times in hours of the specimen which were exposed to 12000 thermal cycles according to temperature profiles depicted in Figure 7. Thereby, the temperatures of the embedded thermocouples with the maximum temperatures were summed up every 10 °C.

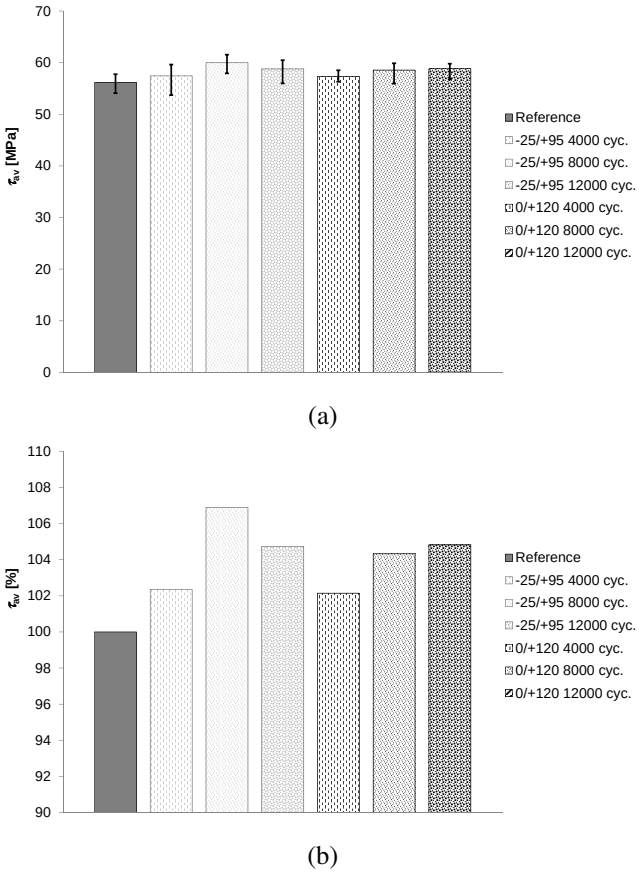

Figure 8. Thermally cycled glass-fibre epoxy (FM906) specimens: (a) absolute values and (b) comparison with the reference (non-cycled) epoxy specimens (cf. Table 1)

Examination of the material properties before and after thermal cycling

For examining the possible changes of the material properties of the glass-fibre prepreg and (heated) GLARE samples, the interlaminar shear strength (ILSS) was tested using the ASTM standard test method for short-beam strength of polymer matrix composite materials and their laminates.[3] The ILSS specimen dimensions for the approximately 2 mm thick specimens were 4 mm x 20 mm. Microscopic imaging was used to study the aluminium-epoxy and the fibre-epoxy interfaces before and after thermal cycling. Heat capacity tests were conducted to investigate the possible microstructural changes of the epoxy. Finally, an ultrasonic C-scan imaging was used to examine delaminations and pores before and after thermal cycling.

The Figures 8 to 10 show the results of the ILSS tests before and after thermal cycling. The Figures a show the average absolute values and the scatter range of the five ILSS tests which were conducted per configuration. The Figures b show the changes of the average material properties compared to the average value of the non-cycled (reference) specimens.

The average ILSS value of the non-cycled glass-fibre epoxy specimens (Reference, GE0) was 56.1 MPa with a scatter of -2 MPa / +1.7 MPa (cf. Figure 8). The average absolute ILSS value of the glass-fibre epoxy specimens increased by 2.3 % after 4000 cycles (GE1), by 6.9 % after 8000 cycles (GE2) and by 4.7 % after 12000 cycles (GE3) for a temperature range of -25 °C to +95 °C. Figure 7 a shows the corresponding temperature profile. Similarly to this, the average absolute ILSS value of the glass-fibre epoxy specimens increased after 4000 cycles (GE4) by 2.1 %, after 8000 cycles (GE5) by 4.3 % and after 12000 cycles (GE6) by 4.8 % for a temperature range of 0 °C to +120 °C. Figure 7 b depicts the associated temperature profile. Hence, the ILSS values of the glass-fibre epoxy specimens tend to increase slightly due to the thermal cycling.

The five non-cycled GLARE specimens (Reference, GL0) showed an average absolute ILSS value of 73.6 MPa with a scatter of -2.8 MPa / +2.9 MPa (see Figure 9). The average absolute ILSS value decreased after 4000 cycles (GL1) by 3.1 % and after 8000 cycles (GL2) by 2.0 %, but increased after 12000 cycles (GL3) by 4.2 % for a temperature range of -25 °C to +95 °C. Consequently, the

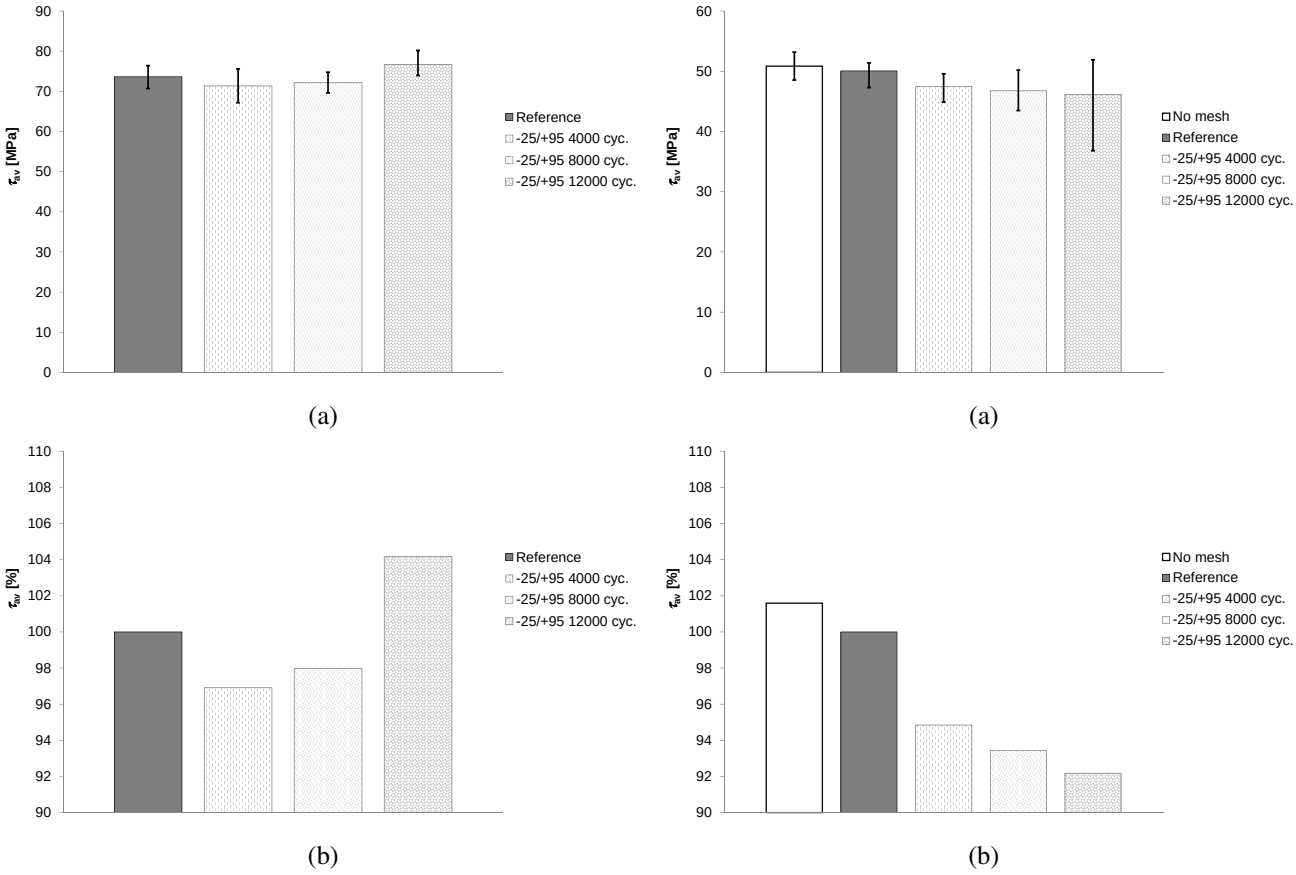

Figure 9. Thermally cycled GLARE 5-3/2-0.3 specimens: (a) absolute values and (b) comparison with the reference (non-cycled) GLARE 5-4/3-0.3 specimens (cf. Table 1)

Figure 10. Thermally cycled heated GLARE 5-2/1-0.3 specimens: (a) absolute values and (b) comparison with the reference (non-cycled) heated GLARE 5-2/1-0.3 specimens (cf. Table 1)

average de- and increases of the ILSS values after thermal cycling with the temperature profile depicted in Figure 7 c almost lie within the scatter range (-3.8 % / +4.0 %) of the non-cycled (reference) specimen.

Figure 10 a shows the average absolute and relative values of the ILSS tests of GLARE 5-2/1-0.3 (No mesh), heated GLARE 5-2/1-0.3 specimens before (Reference, HG0) and after 4000 (HG1), 8000 (HG2) and 12000 (HG3) thermal cycles with the temperature profile depicted in Figure 7 d. The relative values refer to the non-cycled heated GLARE specimens (Reference). The results show that the ILSS values of the GLARE 5-2/1-0.3 specimens with and without the heater mesh were similar. Nevertheless, the GLARE specimen without mesh shows an 1.6 % higher ILSS value. Thermal cycling of the specimens between $-25°$C and $+95°$C increased the scatter and lead to a reduction of the ILSS values by 5.1 % after 4000 cycles, by 6.6 % after 8000 cycles and by 7.8 % after 12000 cycles (see Figure 10 b).

Microscopy investigations were conducted to examine all materials and their interfaces with a focus on the epoxy regions. Figure 11 depicts a section of the sample GE3 which was exposed to 12000 thermal cycles and a temperature range of $-25°$C and $+95°$C (cf. Table 1). The image was made using a scanning electron microscope (SEM) with a magnification of 4000. Neither visually assessable cracks or voids nor visible changes in the fibre-epoxy interfaces due to thermal cycling could be detected. The same results were found when investigating the GLARE and heated GLARE specimens.

Figure 12 shows optical microscope images with magnifications of 100 and 400 of two ILSS specimens, one before (a, c, d) and one after the ILSS test (b). Both specimens were parts from the sample HG3 which was exposed to 12000 thermal cycles and a temperature range of -25 °C and +95 °C (cf. Table 1). No visually detectable defects were found after thermal cycling in the epoxy or in the interfaces between the aluminum (1) and the neighboring 90 ° UD-layers (2) and the copper mesh (5). Furthermore, the ultrasonic C-scan results showed neither delaminations nor pores before and after thermal cycling.

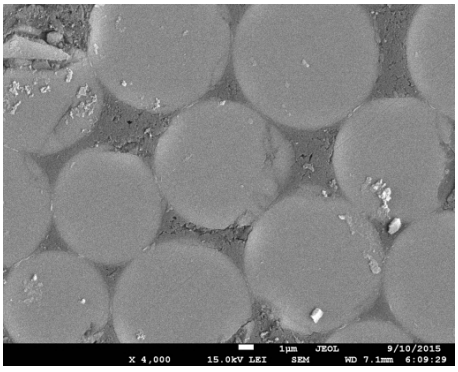

Figure 11. Fibre-epoxy interface: SEM image with a magnification of 4000 of sample GE6

Figure 12 c indicates that zones with no fibres (4) form in the regions between the embedded heater mesh (5) during the curing process. As the copper mesh was embedded between two UD-layers with fibres in the 0 °-direction (3). Furthermore, Figure 12 d shows that the adhesive with which the copper mesh was treated penetrates the epoxy of the neighboring UD-layers (3). The number (6) depicts the embedding resin.

Heat capacity tests were performed to investigate possible changes in the molecular structure of the cycled glass-fibre epoxy samples which indicate ageing. The results are shown in Figure 13 for both the 0 °C to 120 °C and the -25 °C to +95 °C temperature range and compared to the non-cycled reference. Specimens were taken from the center and include one of the sample surfaces.

The reference specimen shows a steady increase in the heat flow near the glass transition region. The cycled specimens show heat flow peaks at higher temperatures in both cases. This is an indication of ageing of the epoxy due to the elevated temperatures[21] during thermal cycling (cf. Table 2). No clear correlation is found however between the amount of cycles and the magnitude and temperature shift of the heat flow peak. The curves are not completely smooth either, which is thought to be caused by the presence of the glass-fibres.

Discussion

The thermal cycling machine

The new trend of developing multifunctional materials with embedded heater elements rises the challenge of simulating thermal fatigue on laboratory scale even more. However, the introduced thermal cycling machine covers the thermal cycling with adjustable temperature profiles of materials with and without embedded heater elements.

The introduced thermal cycling machine enables external heating and external cooling with adjustable temperature

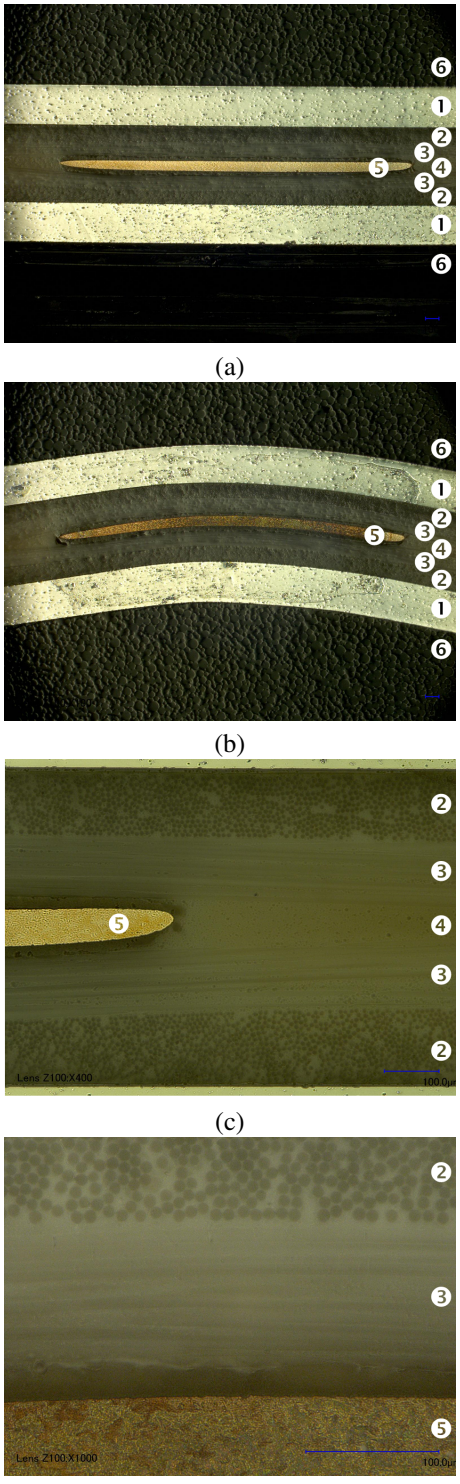

Figure 12. Optical microscope image of a heated GLARE ILSS specimen after 12000 cycles (HG3) and a magnification of 100 of the (a) mechanically non-loaded part and (b) mechanically loaded part. Details of the copper element from subfigure (a) with magnifications of (c) 400 and (d) 1000. The regions (1) to (6) are explained in the text.

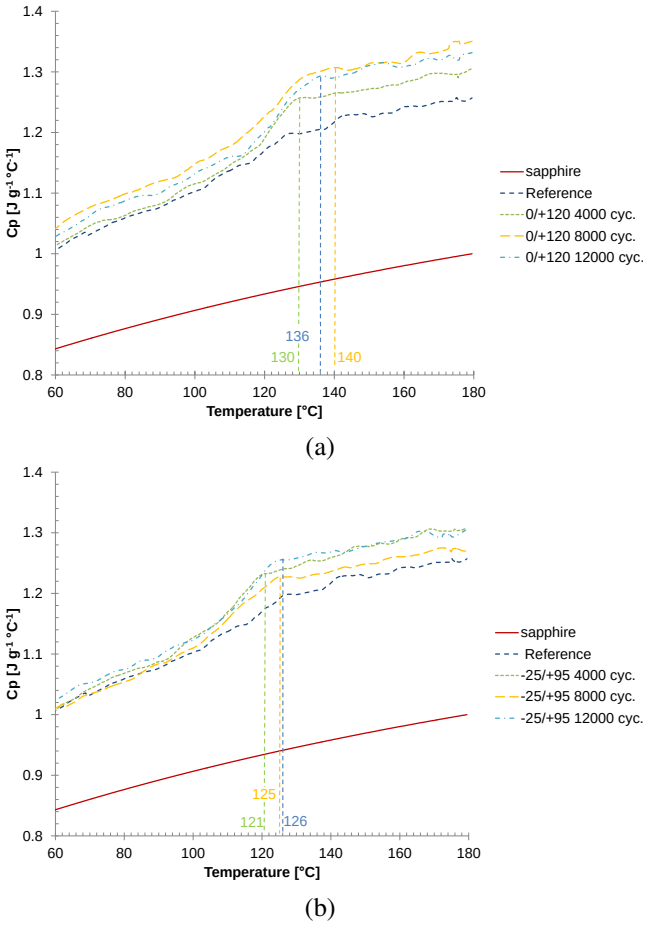

Figure 13. Heat capacity tests of the thermally cycled glass-fibre epoxy specimens compared to the non-cycled reference in the temperature range (a) 0 to 120 °C and (b) -25 to +95 °C.

profiles (heating and cooling rates) by using Peltier elements on both sides of the specimen. Thermal cycling of specimens with heater elements is possible by resistance heating of the internal (embedded) mesh. The heating and cooling powers, the maximum and minimum temperatures and the dwell times (when simulating anti-icing conditions) for both operational conditions can be adjusted independently as two power supplies are used (one for the Peltier elements and one for the embedded mesh) and the out- and input parameters can be adjusted separately. Furthermore, using Peltier elements brings the advantage that no additional liquids are used which might affect the results[24]. To ensure that no moisture from the surrounding air is taken up at low temperatures, the specimens could be additionally wrapped in vacuum bags.

The small dimensions of the thermal cycling machine and its modular design add further flexibility in regard to temperature profiles and facilitate a wider range of applications. For temperature profiles which require lower minimum or higher maximum temperatures and larger temperature change rates the thermal cycling machine can be adapted by positioned it in a climate chamber or by stacking Peltier elements[19;33]. Furthermore, the specimen dimensions can be adjusted by adding or removing Peltier elements and multiple specimens with different (thermal) load histories can be thermally cycled parallel.

However, measures need to be taken to avoid the overheating of the thermal cycling machine for too large heating and cooling powers. The maximum heating and cooling powers are limited by the amount of heat which can be transferred (mainly) via the heat sinks to the surrounding air. Choosing an adequate cooling power and monitoring the heat sink temperatures to avoid overheating of the system are essential. As the Peltier elements cool at one side while they heat at the other side and the Peltier elements are less effective in cooling as in heating[33].

Due to the fact that the Peltier elements and the heater element generate temperature differences, (no absolute temperatures) and the finite specimen thickness (different temperatures across the thickness), the temperatures in the specimens have to be monitored at several positions through the specimen. This is important as different cooling and heating powers generate more or less inhomogeneous temperatures through the thickness for materials with different thermal properties. Monitoring the in-plane temperature profile of the specimen is essential when using the heater mesh for internal (local) heating.

An additional future feature of the thermal cycling machine could be to impose (constant) mechanical stresses to the specimen during thermal cycling. This feature could be important as it can simulate the mechanical and thermal flight conditions. Furthermore, superimposing mechanical stresses and thermal stresses is likely to change the thermal fatigue behaviour of the investigated materials. However, the heating phase using the internal heating is expected to match the time and power used for aircraft de-icing systems. The required time to keep it above a certain temperature is not known in detail as it is affected by the icing conditions like the air flow velocity, humidity and temperature. In future research the amount of cycles will be expanded and the effect of the cycling time will be examined.

Effect of thermal cycling on the material properties

The typical heating curves and the temperature distributions of the tested specimens and materials differ. The main reason for different in-plane temperature distributions is that the heating was performed externally (glass-epoxy and GLARE) and internally (heated GLARE). The main reason for different out-of-plane temperature distributions are the different boundary conditions, thermal properties

and thicknesses of the tested materials. As the electrical power for operating the Peltier elements was similar for all specimens, but the temperature differences of the surrounding air and the minimum specimen temperatures differed. Furthermore, the thermal material properties of the glass-fibre epoxy samples and the GLARE samples differ significantly[13]. The heat capacity of aluminium. is considerably higher than the heat capacity of the glass-fibre epoxy The same statement can be made for the thermal conductivity. Thus, the heat is transferred faster and spread more evenly through the aluminium layers but it needs more heat to reach the same temperature compared to e. g. a glass-fibre epoxy sample.

Test results after thermal cycling showed that the material properties were affected by thermal cycling. The increased ILSS values of the thermally cycled specimens (see Figure 8 and 9) can be explained by ageing which was indicated by the heat capacity tests shown in Figure 13. The heat flow peaks are endothermic peaks and occur in the glass transition regions. These local heat flow peaks and the increased curves indicate ageing due to thermal cycling[21]. The thermally cycled specimens were exposed to elevated temperatures for several hours (see Table 2). Aged epoxy specimens show increased stiffness and strength values. However, the microstructure changes and the ductility decreases. Furthermore, no changes of the physical properties could be detected using an ultrasonic C-scan machine of microscopic imaging.

The decrease of the ILSS values of heated GLARE due to thermal cycling (see Figure 10) is expected to result from the relatively high local stresses introduced by the heater elements during the internal heating phase[20]. The local stresses are a consequence of the different temperature expansion coefficients and the locally high heating rates at the heater element. Especially in the beginning of the heating cycle, the temperature increase rates are high (cf. Figure 7 d) and thus cause significant temperatures differences of the heater element and the surrounding material. Furthermore, those high local thermal stresses arise at times when thermal residual stresses from manufacturing are highest due to the lowest temperatures. One idea to decrease these thermal stress peaks, is to reduce the heating power at the beginning of each heating phase.

Conclusions

The designed and built thermal cycling setup is unique in its kind and capable of performing different types of thermal cyclic testing. The setup has been used to thermally cycle samples with (internal heating and external cooling) and without (external heating and external cooling) integrated heater elements. Thermal cycling times of 60 s to 90 s for temperature ranges of 120 °C were achieved for glass-epoxy composite and (heated) GLARE samples.

Test results after thermal cycling showed that the ILSS values slightly increased after 12000 cycles for the externally heated and cooled glass-epoxy composite and GLARE samples. However, the internally heated and externally cooled heated GLARE samples showed a constant decrease of the ILSS with an increasing number of cycles (-7.8 % after 12000 cycles). Furthermore, embedding the heater mesh in GLARE reduces the ILSS about 1.6 %.

The changes of the ILSS values are likely to result from changes in the microstructure. As microscopic investigations and ultrasonic C-scan results after thermal cycling showed no changes in the physical structure such as cracks or delaminations. Furthermore, heat capacity tests of the glass-fibre epoxy composite samples revealed slightly higher heat flow peaks for increasing numbers of cycles. This indicates ageing of the epoxy due to thermal cycling.

Acknowledgements

This study is funded by the Dutch Technology Foundation STW and Fokker Aerostructures.

References

1. Alderliesten R C, Hagenbeek M, Homan J J, Hooijmeijer P A, De Vries T J and Vermeeren C A J R (2003) Fatigue and Damage Tolerance of Glare, Applied Composite Materials 10, p.223-242.
2. Anisimov A G, Müller B, Sinke J and Groves R M (2015) Strain characterization of embedded aerospace smart materials using shearography, Proceedings SPIE 9435, paper 943524.
3. ASTM, Standard Test Method for Short-Beam Strength of Polymer Matrix Composite Materials and Their Laminates, ASTM standards, D2344/D2344M-13.
4. Botelho E C, Almeida R S, Pardini L C, Rezende M C (2007) Elastic properties of hygrothermally conditioned Glare laminate. Int. J. Eng. Sci. 45, p.163-172.
5. Botelho E C, Rezende M C, Pardini L C (2008). Hygrothermal effects evaluation using the Iosipescu shear test for Glare laminates. J. Braz. Soc. Mech. Sci. Eng. 30, p.213-220.
6. Chilingarov A (2013) Operation of two stacked Peltier elements, Journal of Instrumentation, 8, p.1-12.
7. Costa A A, da Silva D F N R, Travessa D N, and Botelho E C (2012) The effect of thermal cycles on the mechanical properties of fibre metal laminates, Materials and Design, 42 (1), p.434-440.
8. Federal Aviation Administration (FAA) (2010), Airplane and Engine Certification Requirements in Supercooled Large Drop, Mixed Phase and Ice Crystal Icing Conditions, Federal Register 75 (124), 37311-37339.
9. Fibre Metal Laminates Centre of Competence, http://www.fmlc.nl, accessed 9.2.2015

10. Gabb T P, Gayda J and Mackay R A (1990) Isothermal and Nonisothermal Fatigue Behavior of a Metal Matrix Composite, Journal of Composite Materials, 24, p.667-686.
11. Gale M S and Darvell B W (1999) Thermal cycling procedures for laboratory testing of dental restorations, Journal of Dentistry, 27, p.89-99.
12. Hagenbeek M, Van Hengel C, Bosker O J and Vermeeren C A J R (2003) Static Properties of Fibre Metal Laminates, Applied Composite Materials 10, p.207-222.
13. Hagenbeek M (2005) Characterisation of Fibre Metal Laminates under Thermo-mechanical Loadings, PhD thesis, TU Delft.
14. Knobloch L A, Gailey D, Azer S, Johnston W M, Clelland N and Kerby R E (2007) Bond strengths of one- and two-step self-etch adhesive systems, The Journal of Prosthetic Dentistry, 97 (4), p.216-222.
15. Krammer P and Scholz D (2009) Estimation of Electrical Power Required for Deicing Systems, Technical Note, Hamburg University of Applied Sciences, Aero_TN_Deicing_09-07-14, p.1-42.
16. Kulkarni M R and Brady R P (1997) A model of global thermal conductivity in laminated carbon/carbon composites, Composite Science and Technology, Vol. 57, p.277-285.
17. Liu M, Saman W and Bruno F (2012) Review on storage materials and thermal performance enhancement techniques for high temperature phase change thermal storage systems, Renewable and Sustainable Energy Reviews, 16, p.2118-2132.
18. Mohseni M, and Amirfazli A (2013) A novel electro-thermal anti-icing system for fiber-reinforced polymer composite airfoils, Cold Regions Science and Technology, 87, p.47-58.
19. Müller B, Teixeira De Freitas S and Sinke J (2015) Thermal cycling fiber metal laminates: Considerations, test setup and results. In: *Proc. of the* 20^{th} *Int. Conf. on Composite Materials (ICCM)*, Copenhagen, Denmark, 2015, paper no.4212-3, p.1-11.
20. Müller B, Anisimov A G, Sinke J and Groves R M (2015) Thermal strains in heated fibre metal laminates. Proc. of the 6^{th} Int. Con. on Emerging Technologies in Non-destructive Testing (ETNDT), p.1-6.
21. Odegard G M and Bandyopadhyay A (2011) Physical Aging of Epoxy Polymers and Their Composites, J. of Polymer Science Part B: Polymer Physics, 49 (24), p.1695-1716.
22. Pacchione M and Telgkamp J (2006) Challenges of the metallic fuselage, Proceedings of the 25^{th} International congress of the aeronautical sciences (ICAS), p.1-12.
23. Pang J H L, Chong D Y R and Low T H (2001), Thermal Cycling Analysis of Flip-Chip Solder Joint Reliability, IEEE transactions on components and packaging technologies, 24 (4), p.705-712.
24. Park S Y, Choi W J, and Choi H S (2010) The effects of void contents on the long-term hygrothermal behaviors of glass/epoxy and GLARE laminates, Composite Structures 92 p.18-24.
25. Qi Y, Lam R, Ghorbani H R, Snugovsky P and Spelt J K (2006) Temperature profile effects in accelerated thermal cycling of SnPb and Pb-free solder joints, Microelectronics Reliability, 46, 2006, p.574-588
26. Shih H C, Ho N J and Huang J C (1996) Precipitation Behaviours in Al-Cu-Mg and 2024 aluminium Alloys, Metallurgical and materials transactions A, 27, p.2479-2494.
27. Shimokawa T, Katoh H, Hamaguchi Y, Sanbongi S, Mizuno H, Nakamura H, Asagumo R, Tamura H (2002) Effect of Thermal Cycling on Microcracking and Strength Degradation of High-Temperature Polymer Composite Materials for Use in Next-Generation SST Structures, Journal of Composite Materials, 36 (7), p.885-895.
28. Sinnett M (2007) 787 No-Bleed Systems: Saving Fuel and Enhancing Operational Efficiencies. Aero Quarterly QTR_04 | 07, p.6-11.
29. Sinke J (2003) Manufacturing of GLARE Parts and Structures, Applied Composite Materials 10, Kluwer Academic Publishers, p.293-305.
30. Stickley G W and Anerson H L (1956) Effects of Intermittent Versus Continuous Heating upon the Tensile Properties of 2024-T4, 6061-T6 and 7075-T6 Alloys, NACA technical memorandum 1419, p.1-8.
31. Vermeeren C A J R, Beumler Th, De Kanter J L C G, Van der Jagt O C and Out B C L (2003) Glare Design Aspects and Philosophies, Applied Composite Materials 10, p.257-276.
32. Vlot A and Gunnink J W, eds. (2001) Fibre metal laminates: An introduction. Kluwer Academic Publishers. Dordrecht. The Netherlands.
33. Wijngaards D D L, Cretu E, Kong S H and Wolffenbuttel R F (2000) Modelling of integrated Peltier elements, Proceedings of the 3rd International Technical Conference on Modelling and Simulation of Microsystems, p.652-655.
34. Ypma M S (2001) Overview of tests concerning the influence of temperature and environmental exposure on Glare. Report B2V-00-41, Glare Research Program, Delft.